



POLITECNICO
MILANO 1863

[RE.PUBLIC@POLIMI](#)

Research Publications at Politecnico di Milano

Post-Print

This is the accepted version of:

G. Sala, L. Di Landro, A. Airoidi, P. Bettini
Fibre Optics Health Monitoring for Aeronautical Applications
Meccanica, Vol. 50, N. 10, 2015, p. 2547-2567
doi:10.1007/s11012-015-0200-6

This is a post-peer-review, pre-copyedit version of an article published in Meccanica. The final authenticated version is available online at: <https://doi.org/10.1007/s11012-015-0200-6>

Access to the published version may require subscription.

When citing this work, cite the original published paper.

Permanent link to this version

<http://hdl.handle.net/11311/961255>

Fibre Optics health monitoring for aeronautical applications

Giuseppe Sala · Luca Di Landro · Alessandro Airoidi · Paolo Bettini

Received: date / Accepted: date

Abstract The detection of stress/strain field in structural components represents one of the cornerstones of continuous mechanics analysis of materials and structures. In particular, this paper presents some of the most remarkable aspects of aeronautical structures monitoring techniques through fibre optics (FO) sensors; given their capability to convert local or distributed strains into optical signal and to transmit it remotely, optical fibres represent a powerful detection tool which can be integrated in complex structures. Firstly, some basic technological concerns to be tackled in view of sensors integration are considered, e.g. trade-off process between bonding and embedding techniques, co-bonding or co-curing, inter- or intra-laminar embedding, compatibility between host material and optical fibres, degree of invasivity and interface analysis, bending sensitivity, use of quick-packs and connectors to guarantee sensors integrity and functionality. Then, general concerns to be faced during the design process of sensors networks for strain sensing, health- and process-monitoring are analysed (e.g. distributed, localized and co-located sensors, hot-spot identification, signal management, multiplexing, attenuation). Moreover, a number of issues are addressed for a reliable conversion of optical signal into mechanical strain field. In particular, theoretical and experimental techniques are presented, devoted to thermal/mechanical signals decoupling. Finally, the use of fibre Bragg's grating (FBG) sensors and chirped arrays are compared in view of solv-

ing the problem of reconstructing the stress/strain field on the basis of spectral signals provided by FO sensors.

Keywords Aeronautical structures · health monitoring · process monitoring · strain sensing · fibre optics sensors · integration techniques

1 Introduction

Nowadays, structural health monitoring represents one of the major concerns for modern aeronautical structures maintenance and aircraft fleet management. As a matter of fact, the progressive ageing of the aircraft

Abbreviations

ACT	across capillary tube
DCB	double cantilever beam
DTG	draw tower array
ECT	extremity capillary tube
ENF	end notched flexure
FO	fibre optic
FBG	fibre bragg grating
FWHM	full width half maximum
GFRP	glass fibre reinforced plastic
IFSS	interfacial shear stress
MAXERR	maximum error
QP	quick-pack
RMSE	root mean square error
RTM	resin transfer moulding
SHM	structural health monitoring
SpaC	spatial continuity
SpaD	spatial discontinuity
SpeC	spectral continuity
SpeD	spectral discontinuity
TMM	transfer matrix method
UD	unidirectional

G. Sala · L. Di Landro · A. Airoidi · P. Bettini (✉)
Politecnico di Milano, Dipartimento di Scienze e Tecnologie
Aerospaziali, Via La Masa 34 20156 Milan, Italy
Tel.: +39-02-23998391
Fax: +39-02-23998331
E-mail: paolo.bettini@polimi.it

1 fleet can make questionable their durability, affordabil-
 2 ity and profitability, as well as the real effectiveness of
 3 conventional preventive maintenance philosophy, based
 4 on a scheduled-based approach and non-destructive in-
 5 spection techniques. Such uncertainties become even
 6 more alarming when the structures are made of or-
 7 thotropic and inhomogeneous composite materials. The
 8 ageing of modern *damage tolerant* composites aereo-
 9 nautical structures should be better managed through
 10 predictive maintenance philosophy, sometimes based on
 11 condition-based approaches; the effect of operational
 12 loads, unexpected events and damages on the mechani-
 13 cal response of structural components must be promptly
 14 recorded so that proper actions can be activated. This
 15 requires the integration of a network of sensors, ac-
 16 tuators and detection algorithms, synergistically cou-
 17 pled with continuum mechanics, fracture mechanics and
 18 damage mechanics techniques. The structures become
 19 *smart structures* and the philosophy is called structural
 20 health monitoring, usually implemented in modern air-
 21 craft through health and usage monitoring systems. Such
 22 methodology is very promising and is going to be adopted
 23 by most modern aircraft, provided some ma-jor concerns
 24 are successfully tackled: sensors and actua-tors
 25 integration, data processing and storage, noise and false
 26 signals filtering, environmental and variable op-erational
 27 conditions management. In brief, structural health
 28 monitoring (SHM) systems can be successfully used,
 29 provided reliability, availability, maintainability and
 30 safety requirements are satisfied. Due to their adapt-able
 31 shape and small size, FOs are suited to be easily
 32 embedded in composite laminates with limited inva-
 33 sivity and sensitivity to environmental degradation [5].
 34 The presence of closely spaced FBGs inscribed on FOs
 35 produces a wavelength change of transmitted/reflected
 36 light according to strain induced spacing variation. FBGs
 37 are thus accurate local strain sensors with extremely
 38 small dimensions. Moreover, FBG sensors, normally in-
 39 scribed on FOs, are immune to electromagnetic fields, are
 40 able to transduce several physical quantities (by di-rect
 41 or indirect measurements) and present multiplex-ing and
 42 real time capabilities [19].
 43 These latter features are often extremely valuable for
 44 practical applications, since they allow the fast and
 45 reliable transmission of a large number of data. As a
 46 matter of fact, a complex architecture of sensors can be
 47 designed and implemented in a structure, which is able to
 48 monitor deformations in a number of differ-ent locations
 49 and directions. In particular, a special kind of sensors,
 50 characterized by a variable-pitch grat-ing (chirped) are
 51 particularly appealing, since, once a code for the
 52 numerical simulation of their reflected spec-trum is
 53 developed, the strain profile along the sensor

can be reconstructed. Such devices show a one-to-one
 correspondence between reflected spectrum wavelength
 and strain distribution along the sensor, making chirped
 gratings ideal for strain sensing over extended lengths
 ($\leq 80\text{-}100$ mm) [2-4], while their use for real time mon-
 itoring is prevented, being data post-processing needed
 to reconstruct the strain profile acting on the sensor. An
 additional type of devices, called Draw Tower Grat-ing
 arrays, can be conveniently adopted as well, each one
 having different spectral and spatial characteris-tics.
 These arrays are produced through an innovative
 technique, where gratings are inscribed directly after
 spinning on the draw tower, before coating deposition.
 Such sensors do not require fibre stripping and recoat-
 ing, so maintaining high tensile strength and reliability
 [12, 21, 17]. Moreover they are cheaper than conven-
 tional arrays and their spectral characteristics can be
 easily tuned for obtaining the most disparate spectral
 shapes and sensor responses.
 Besides monitoring-diagnosis-prognosis issues, further
 crucial aspects of health and usage monitoring systems
 need to be considered in view of their reliable industrial
 adoption [8]. In particular, one should take into account
 that simultaneous mechanical and thermal stimuli in-
 duce effects which interact and overlap, thus affecting
 FBGs response. Such a phenomenon prevents a prompt
 interpretation of FBGs signals. The need of discrimi-
 nating thermal and mechanical strain contributions has
 promoted the development of optical signals decoupling
 techniques [9].

2 General consideration about FO sensors networking

Prior to start dealing with the specific sensors inte-
 gration concerns (e.g. bonding vs. embedment, inter-
 face efficiency, static and fatigue invasivity), general
 issues related to the design of sensors network must be
 faced. This implies the consideration of more gen-eral
 and higher-level problems, correlated with the net-work
 topology and the system overall efficiency, relia-bility,
 durability, affordability. These aspects do not de-pend
 on the system specific finalization, so they indiffer-ently
 apply to usage monitoring (for strains, loads, tem-
 perature, moisture content measurement, etc.), health
 monitoring (for the investigation of damage mechan-ics
 parameters and subsequent diagnosis and prognosis
 phases) and process monitoring (devoted to the evalua-
 tion of curing conditions, infusion parameters and resid-
 ual stresses onset during fabrication, as well as loading
 and heating during machining of composite materials).

1 Preliminarily, a basic choice between *distributed* acqui-
2 sition through long *chirped* sensors or particular optical
3 architectures (e.g. Brillouin) and *point-to-point* discrete
4 local sensing should be made. Advantages and disad-
5 vantages of the two solutions should be compared as
6 well, taking into account, for example, the need of ref-
7 erence baselines in the first case and of efficient interpo-
8 lating algorithms in the second one. Besides, an efficient
9 and synergistic correlation with FEM analysis should be
10 pre-defined: as a matter of fact, an accurate identifi-
11 cation of *hot-spots* allows to selectively densify the
12 sensors distribution, reducing in the same time their to-
13 tal numbers, as well as the complexity, the burdensome
14 management and the weight/cost of the whole system.
15 Moreover, it is well known that FO systems are also
16 particularly convenient thanks to their capability to
17 manage several sensors lying on the same fibre, exploit-
18 ing efficient multiplexing techniques. Among the others,
19 *wavelength division multiplexing* and *time division mul-*
20 *tiplexing* techniques can be conveniently adopted, once
21 respective pros and cons are compared: wavelength di-
22 vision multiplexing technique can acquire continuously
23 and contemporarily a certain number of different sen-
24 sors irrespectively of their pitch, provided such a num-
25 ber is not too large. On the contrary, time division
26 multiplexing technique allows the use of several (up to
27 100) identical sensors inscribed on a single fibre, but the
28 mutual distance between two adjacent sensors must be
29 large enough to allow the optical interroga-tor to
30 discriminate among different signals, being the
31 acquisition sequential. As a consequence, wavelength
32 division multiplexing technique is particularly suited for
33 accurate and dynamic local monitoring of relatively
34 small areas, while time division multiplexing technique
35 can be conveniently adopted in case of large structures
36 quasi-statically loaded. A further basic aspect, deserv-
37 ing particular attention, is optical attenuation, since it
38 can affect the signal-to-noise ratio. Optical attenuation
39 depends on intrinsic characteristics of both core and
40 cladding, which should be chosen having also this crite-
41 rion in mind (e.g. poly-acrylate coatings perform better
42 than poly-imide ones). On the other hand, attenuation
43 depends on some features of the whole system such as
44 the number of splice joints and connectors. It also de-
45 pends on FOs bending (and micro-bending) sensitivity,
46 that is affected by the relative orientation between FOs
47 and fiber reinforcement: attenuation increases if sensors
48 are embedded between off-axis unidirectional and fab-
49 ric layers, while it is minimized when adjacent layers
50 consist of on-axis unidirectional.
51 Another general concern, affecting most FO sensors net-
52 works, descends from thermal and mechanical coupling.
53 Sometimes, temperature measurement through thermal

strains represents the main goal of the system (e.g. usage
monitoring, process monitoring). In other cases thermal
and mechanical effects should be decoupled: several
strategies have been developed, some of which will be
presented in the following. However, stringent
requirements, need of simple and fast placement, to-
gether with inherent difficulties related to the capabil-
ity of transferring signals through moving components,
may limit the choice of the decoupling techniques which
can be adopted. A typical situation where design is-sues
and technological requirements do not allow a free
choice among optical architectures is represented by he-
licopter blades monitoring . As a matter of fact, easy
placement procedure, robustness and need of adopting
commercially available instrumentation to be installed
at the root of rotors blades represent compulsory re-
quirements for an effective implementation.
Finally, in designing the sensors network for setting up a
FO monitoring system, some very basic criteria should
be borne in mind, relevant to its reliability, reparability,
maintainability, complexity, weight and cost. Since such
criteria are very often conflicting, a trade-off procedure
should be devised in order to find out a compromise so-
lution. As an example, reparability and maintainability
are maximized if sensors are bonded to the surface of the
structure, but, so doing, environmental endurance and,
consequently, reliability can be affected. Addition-ally, a
highly-fractionated network of fibres, consisting of
several branches joined through connectors, maxi-
mizes reparability and maintainability, but implies an
increased number of connectors and increases system
complexity, weight and cost. Overall system *robustness*
and *availability* are increased as well, to the expenses of
reliability, which, in turn, is reduced owing to the
increased number of components. In conclusion, a re-
liability, availability, maintainability and safety analy-
sis implementing a global *system engineering* approach
[22] is worth adopting to get a fully comprehensive op-
timal solution.

3 Integration issues

The integration of FO sensors into structural composite
components can be generally achieved in two different
ways, that is bonding them to the external surface or
embedding them inside the laminates during the man-
ufacturing process. External bonding can appear the
simplest and most preferable method, even though the
procedure hides some difficulties, mainly due to FOs
brittleness and small bonding surface. For these rea-
sons, sensors installation becomes burdensome and the
interface with the structure reveals inadequate to en-
sure acceptable strength levels.

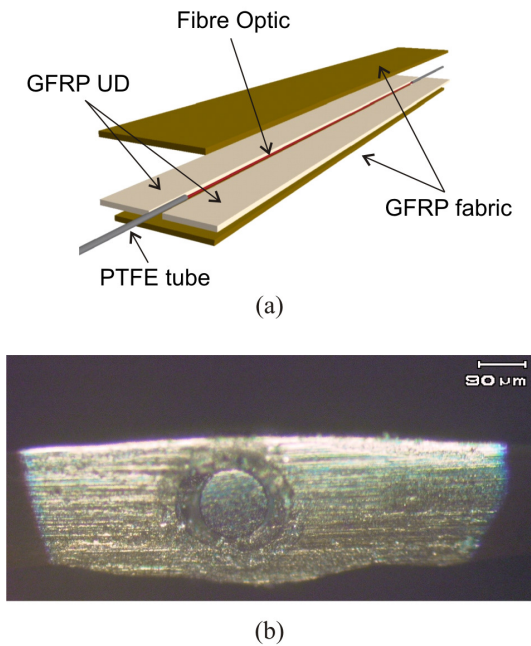


Fig. 1 Quick-Pack production: (a) scheme of the Quick-Pack; (b) micrograph of FO embedded in a laminate showing the core and the coating of the fiber.

In order to overcome these problems, a special device should be adopted, consisting of a thin flexible GFRP laminate embedding FOs (Fig.1a). A dedicated vacuum bag assisted curing cycle minimizes resin loss and voids percentage amount around FO. A "smart" ribbon results, named *Quick-Pack* (QP), in which a well-protected FO is placed. Its flexibility, guaranteed by external fabric plies, allows a perfect adhesion on curved surfaces, while reinforcement fibres of an inner UD layer preserves FO integrity and operation. Besides, QP can be employed at high process temperatures, irrespective of the limited thermal stability of FOs coating (for instance, acrylate coating) (Fig.1b). QPs can be bonded to the surface of composite laminates according to standard *co-bonding* process or directly during the manufacturing of the component itself (*co-curing* process)[8]. The first one consists in a simple procedure relying on low curing temperature paste or film adhesive. In co-curing technique, QPs adhesion is granted by laminate uncured resin: no additional adhesive is required. As a consequence, both QP materials and consumables must comply with (high) curing temperatures of composite part. However, even if more critical, the latter process guarantees higher strain-transfer capability between monitored part and monitoring sensor. A possible drawback can arise, consisting in QP and FO tubing sinking into preregs, which may create undesirable indentations affecting the final laminate (Fig.2). Special

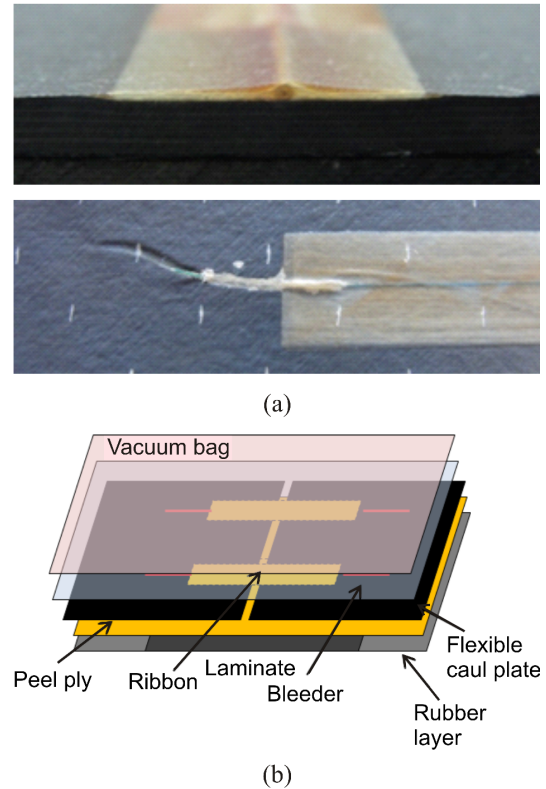
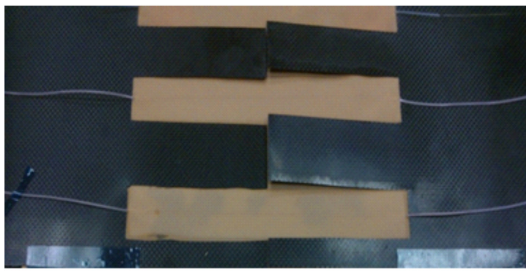
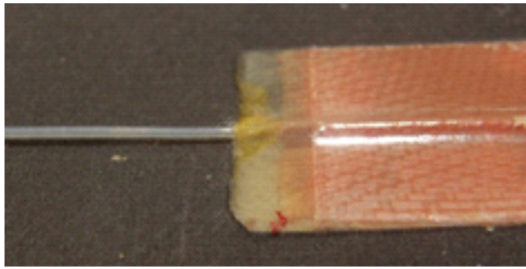


Fig. 2 Co-curing technique: (a) sinking of QP and PTFE tubing and (b) scheme of the developed procedure.

composite caul plates, with the half thickness of the QP, can be applied on the top of uncured laminate (Fig.2b) in order to avoid FO breakage and QP misalignments. Figure 3 shows a detail of these very flexible caul-plates during vacuum bag preparation and the final result at the end of the co-curing process. As an alternative to co-bonding and co-curing techniques, FOs can be embedded inside composite laminates directly during lamination phase: so doing, monitoring is possible at hardly accessible locations and FOs protection is guaranteed from environmental effects. This is particularly relevant if clean and smooth surfaces are required (e.g. aerodynamic surfaces). On the other hand, the development of a proper embedment technique has to address a number of critical issues. The preservation of FO coating polymer integrity during embedment is necessary to ensure homogeneous adhesion between host material and sensor. When peculiar optical architectures are adopted (e.g. FBG), it is of paramount importance to avoid FO cross-section distortions, which could introduce misworking or inaccurate measurements. Both aspects are influenced by host material lamination sequence. In particular, off-axis reinforcing fibres induces local states-of-stress on gratings, possibly leading to permanent alterations of reflected spectrum, or even



(a)



(b)

Fig. 3 Co-curing technique: (a) special carbon fabric caul-plates positioned on the top surface of the laminate before curing cycle and (b) no visible sinking of the QP at the end of the process.

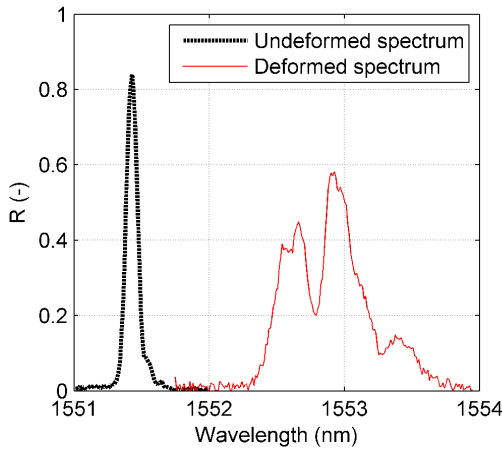
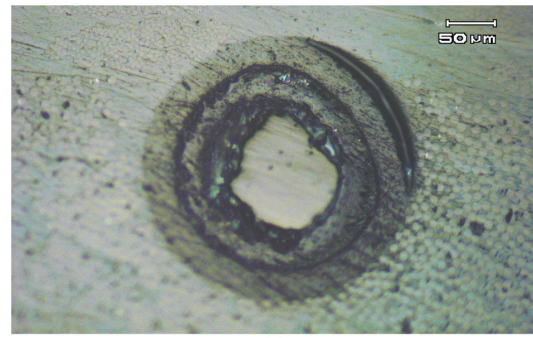


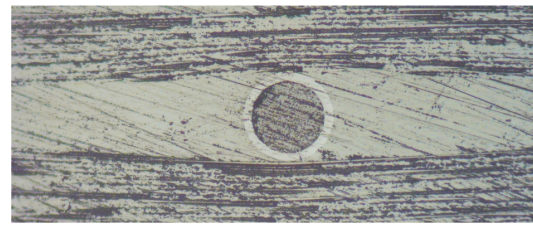
Fig. 4 Effects of a FO deformed cross-section on the reflected spectrum of a Bragg grating sensor.

to the complete loss of functionality of the sensor itself (Fig.4).

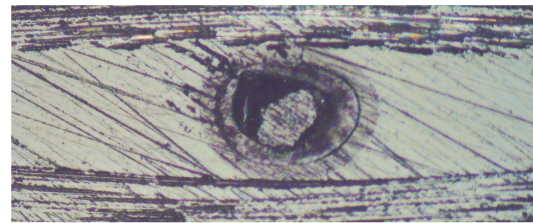
When FOs are directly embedded in cross-ply or angle-ply laminates, microscopy analysis shows standard acrylate coating undergoing relevant deformation due to high curing pressures and temperatures (Fig.5). Consequent alterations of output signal suggest FOs to be embedded between on-axis UD layers. To overcome such a drawback, resistant coatings like polyimide, ceramic or metal, may be used as well. Figure 5 also highlights the presence of resin pockets around FO, that implies ef-



(a)



(b)



(c)

Fig. 5 Effect of the misalignment between FO and reinforcing fibres on coating deformation: no visible effects in case of FO is (a) aligned or (b) in case of polyimide coating is adopted; (c) visible deformation of acrylate coating in an angle-ply laminate.

fects even more serious from the point of view of FO invasivity. Finally, a reduction of optical signal transmission occurs when FOs are subjected to micro-bending phenomena (owing to weaviness of bordering layers): again, the adoption of QPs makes FOs embeddable in any lamination sequence with no effect due to misalignment (Fig.6).

The degree of invasivity related to different embedment techniques (QP vs. direct embedment) can be evaluated through fatigue tests performed on representative structural elements, like a helicopter rotor blade [5]. Two different specimens, have been considered, being FBG sensors respectively embedded along reinforcing fibres (in *spar elements*) and via QP (in *trailing edge elements* where upper and lower blade skins are bonded together) (Fig.7). Sensors performances are evaluated by comparing their outcomes to reference strain gauges signals, to identify possible sensitivity change due to fatigue loads. Besides, endurance analysis comparing the

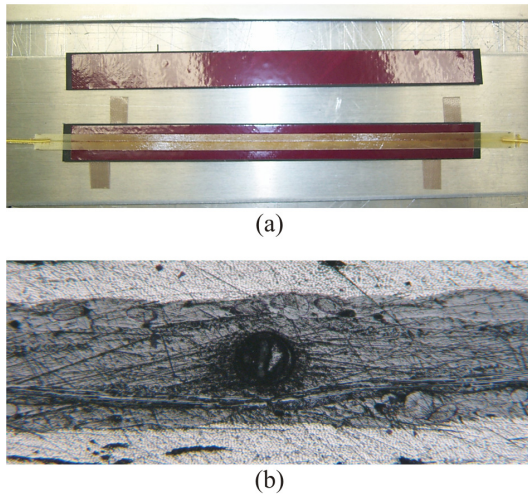


Fig. 6 FO embedment technique through QP (QP embedment): (a) positioning of the QP between two solid adherends and (b) cross section view of final laminate.

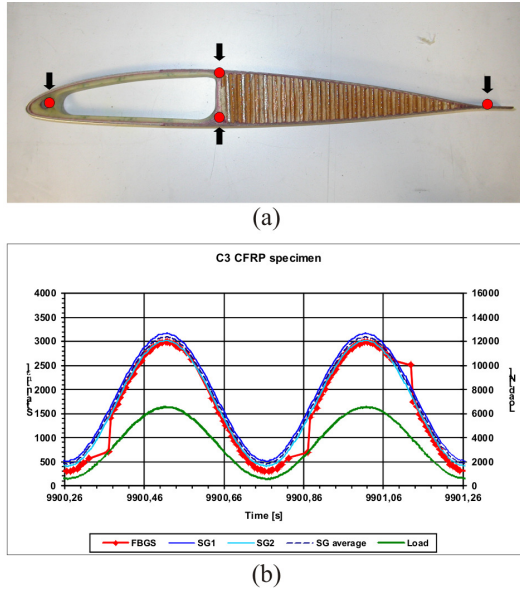


Fig. 7 Invasivity evaluation of FO embedded in composite components: (a) location of hot spots in a cross section rotor blade and (b) example of the sensor response during fatigue tests.

behavior of plain and FO-sensitized specimens allows to point out possible damage onset due to embedded FOs or QPs. As a matter of fact, post-fatigue analysis shows no micro-cracks onset and growth, in spite of 10 million cycles at $f=10\text{Hz}$ frequency, $R = 0.1$ fatigue ratio and max load to about $4000 \mu\epsilon$ [5]. Low invasivity of sensors implies no damaging effect and allows high measuring accuracy.

To get a strong interface between sensors and host material, a crucial role is played by the embedment techniques, as well as by the nature of FO. To evaluate

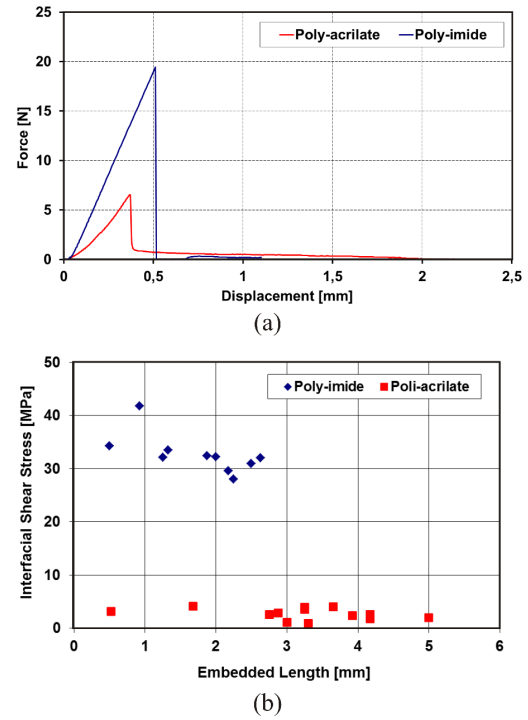


Fig. 8 Comparison between Epoxy resin/FO interfaces (two coatings: poly-acrylate and poly-imide); (a) Pull-Out curves; (b) Inter Facial Shear Stress.

the stress-transfer capability of the interface, pull-out tests should be carried out on different kind of FO coatings. Specimens consist of small resin blocks partially embedding a single fibre (embedded length L shorter than critical value L_C). The latter is defined as the embedded length which gives a pull-out force equal to the fibre failure load: so doing, debonding occurs rather than fibre failure. Pull-out test supplies maximum shear stress through an equilibrium relationship, provided a uniform stress distribution is assumed along the interface [36]:

$$\tau_{IFSS} = \frac{F_{MAX}}{\pi d L} \quad (1)$$

where F_{MAX} is the maximum value of force corresponding to debonding and d is the fibre diameter. A specific testing equipment allowing reliable and repeatable fiber embedment and clamping was designed [7, 6].

Figure 8 and figure 9 respectively show typical force vs. displacement curves and micrographs of polyacrylate- and polyimide-coated FOs. Polyacrylate coatings shows mixed adhesive/cohesive fracture occurring at 2.7 MPa average Interfacial Shear Stress (IFSS); poly-imide specimens collapse implies only adhesive failure, at higher stress levels (IFSS=32.7 MPa).

A potentially advantageous integration technique consists in FOs direct embedment during fabric weaving:

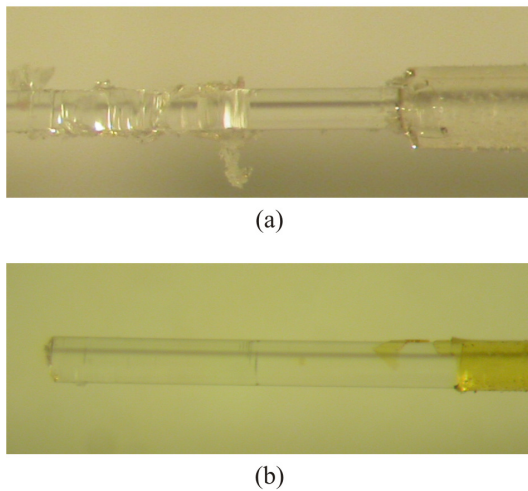


Fig. 9 Comparison between Epoxy resin/FO interfaces (two coatings: poly-acrylate and poly-imide; (a) micrographs of damaged poly-acrylate coating; (b) smooth poly-imide-coated FO cladding after pull-out.

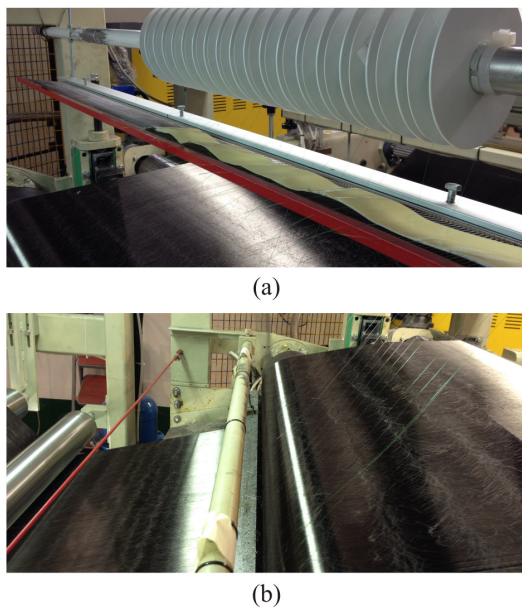


Fig. 10 Intralaminar embedment of FOs during the weaving stage of carbon fibre UD prepreps.

so doing FOs are integrated inside dry lamina reinforcement and are allowed to reduce interlaminar invasivity; interface characteristics are improved as well, thanks to a better interaction with host material. Figure 10 shows the inter-weaving process (preliminary technological assessment).

Irrespective of adopted integration procedure, the weak point of FO health monitoring systems reside in the connection with opto-electronic devices. As a matter of fact, FOs protruding from laminates edges prevent any post-cure machining and imply handling concerns.

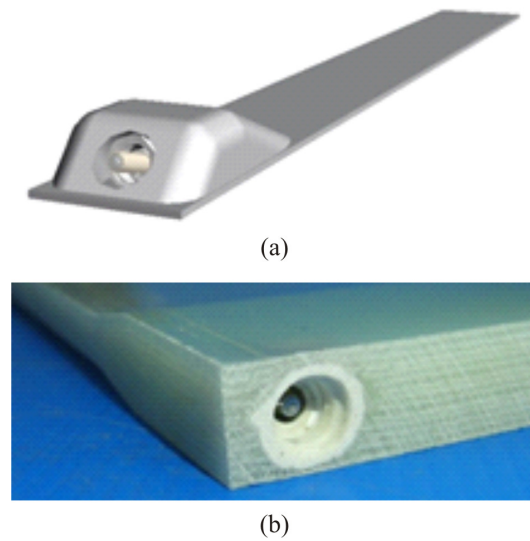


Fig. 11 Conceptual and technological assessment of embeddable FO connectors: (a) quick-pack with end connector and (b) actual embedment in a laminate.

In principle, embeddable connectors could represent a viable solution: FOs featuring such devices may terminate inside the laminate and connect to external opto-electronics once the component installation is accomplished. A promising preliminary technological assessment of embedded connector is shown in figure 11.

4 Load monitoring

In their simplest application, FBG sensors carried by optical fibres can be used to acquire strain measures averaged over the grating length. However, the inherent characteristics of sensor networks based on optical fibres, such as lightness and immunity from electromagnetic jamming, make conceivable the integration of a relatively large number of sensors into a structural component. Such networks will involve a moderate weight cost and could be reliably interrogated in flight conditions at adequate frequencies, so to make possible the reconstruction of the strain field evolution in operative conditions.

The spatial resolution and the level of physical integration of optical fibres into the structures required to extract meaningful information from sensor data depends on the scope of strain sensing. Indeed, if the objective is the identification of internal local damages in a composite structure, such as in the application described in Takeda et al. [35], a very refined network is required and sensors embedded in composite laminates are likely to represent the best choice to detect the signatures of damage on the strain state. Conversely, few strain sen-

sors can be required to approximately know the resultant of the external forces applied to a structure. At an intermediate level, a relatively dense network of sensors can be applied to a structural component to reconstruct the strain field for a more detailed evaluation of the internal stresses and of the stresses transmitted by the surrounding components.

Such level of application becomes particularly interesting for innovative composite and hybrid aircraft structural architectures, which may behave in more complex ways than traditional metallic constructions, under the action of thermo-mechanical loadings. A detailed knowledge of load conditions in the most important structural parts would provide significant information to define and update maintenance operations. Moreover, the availability of a continuous monitoring of the structural response can be exploited to detect the modification of load paths derived from aging, by the presence of damage in redundant parts and by the introduction of new flight configurations. Potential advantages are also related to recent trends towards the application of innovative morphing structures to perform load alleviation and to optimize the shape of aerodynamic surfaces for different missions or mission segments [4], which can increase the variety and the uncertainties of load conditions that can be experienced by the structural components of a flight vehicle.

The reconstruction of the whole strain field in a structural element on the basis of local strains is an inverse problem that can be addressed by methods based on least square approximations [31]. Assuming a linear behavior, the problem can be significantly simplified if the loading conditions applied to the element can be approximated by a set of m parametrized loads, acting at known location in the structures, which are represented by a vector $\{F\}$. Each term of the parametrized load set induces a strain field. Considering a set of n local strains, $\{\varepsilon^*\}$, acquired at given position by the sensor network, the application of a single term F_i of the load vector $\{F\}$ leads to a set of strain values that can be expressed as in Eq. (2), under the assumption of linear response.

$$\{\varepsilon^*\}_i = \{\alpha\}_i F_i \quad (2)$$

where $\{\alpha\}_i$ is a vector of influence coefficients, which provides the local strains for a unit value of the load term F_i . The superposition of all the parametrized loads leads to a vector of strain measures that is expressed by defining a rectangular matrix of influence coefficient, $[\alpha]$, whose columns are the vectors $\{\alpha\}_i$, as indicated

in Eq. (3).

$$\{\varepsilon^*\} = \sum_{i=1}^m \{\varepsilon^*\}_i = [[\alpha]_1 \cdots [\alpha]_i \cdots [\alpha]_m] \{F\} = [\alpha] \{F\} \quad (3)$$

If the matrix $[\alpha]$ is known and the vector of strains $\{\varepsilon^*\}$ is given, the vector of the unknown loads $\{F\}$ can be evaluated by minimizing the squared norm of the distance between the experimentally acquired strains and the strains computed by using $[\alpha]$, as expressed in Eq. (4).

$$\|\{\varepsilon^*\} - [\alpha] \{F\}\|^2 = \sum_{j=1}^m \left(\varepsilon_j^* - \sum_{i=1}^n \alpha_{ij} F_i \right)^2 \quad (4)$$

The minimization of the norm in Eq. (4) leads to a least square problem with the solution expressed in Eq. (5).

$$\{F\} = ([\alpha]^T [\alpha])^{-1} [\alpha]^T \{\varepsilon^*\} \quad (5)$$

Hence, the system of parametrized loads can be identified if the coefficients of influence $\{\alpha\}_i$ are known. Such vectors can be evaluated by experiments or by developing a finite element model of the structural component and by separately applying the F_i loads, on the basis of Eq. (2).

In an aeronautical component, loading conditions can be a generic combination of external loads and of loads transmitted by the surrounding structure. Such load system can be relatively complex, but the knowledge of the basic structural behavior of elements in the stressed skin constructions, which are typically used in aeronautical structures, can provide a guideline to define an acceptable simplified parametrized set of load components.

An example of application is provided considering a part of a wing spar made of carbon/epoxy composite material, subjected to a generic load conditions, endowed with a FBG sensor network for the acquisition of longitudinal strains in each bay, between the ribs. The real-time monitoring of the whole strain field in service should provide information on overloads and potentially safe-critical conditions. The spar segment considered has a C-shape section and a uniform lamination sequence, with about 48% of reinforcement fibres in ± 45 direction, 34% in 0 direction and 14% in 90, being the 0 direction identified by the longitudinal axis of the spar.

The spar segment, which is represented in figure 12a, includes 7 bays, which are separated by ribs. The sensors networks are considered applied along the external surface of the spar, on the flanges and on the web. The FBG sensors are oriented to measure longitudinal

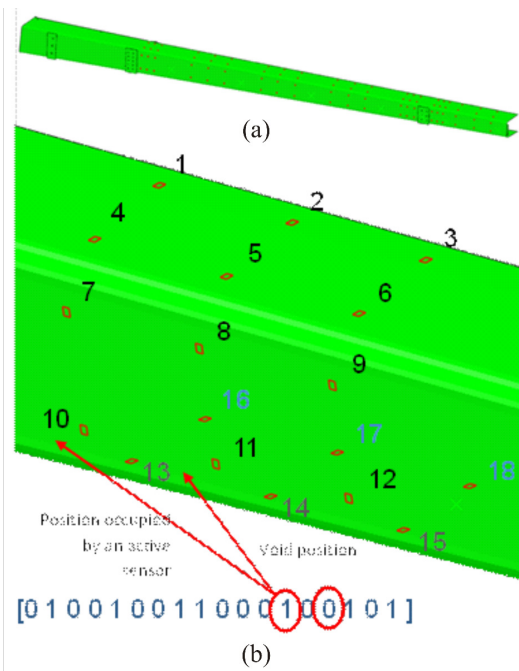


Fig. 12 Active sensors positioning and related codifying vector (typical): (a) full wing spar segment and (b) possible FBG sensors location.

strains in 18 potential positions in the bay. Such installation can be obtained by bonding six QP per bay, of the type defined in the section 3, each one potentially hosting three sensors. The possible locations of sensors are defined in figure 12b. By varying the number and the position of the active sensors, 2^{18} configurations are possible in each bay. Such configurations can be coded in the vector that is shown in figure 12b, where positions hosting an active sensors are represented by a unit value and void positions are indicated by zeros. The sensor network is used to identify a parametrized load system, presented in figure 13, which includes 17 concentrated forces and 12 distributed load systems. The concentrated forces are transmitted to the spar segment in correspondence of the ribs. In the finite element model of the spar such forces are applied by means of rigid plates, which are visible in figure 13 and represent the attachments of the ribs to the internal surface of the spar. The plates are modeled by rigid elements and connected to the web of the spar model by means of rigid bodies in correspondence of the bolts. Concentrated forces include longitudinal and horizontal resultants as well as bending moments. The distributed loads are applied as nodal force systems to the caps of the spar and represent the action transmitted by the panels. They include 8 longitudinal loads, divided into upper and lower components, and 4 systems representing torsional moments. A nominal finite

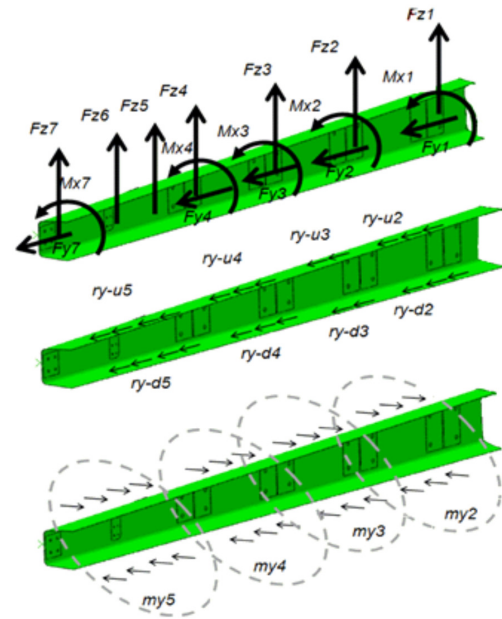


Fig. 13 Generic parameterized load condition.

element model of the spar is clamped at the root and used to calculate the coefficients α_{ij} that provide the longitudinal strain at all the potential positions, ε_j^* , by applying a single component of the parametrized load system F_i . A study is performed to evaluate the performance of the load identification system for various configuration of sensor networks, assuming an identical configuration in all the bays, with n_b active sensors per bay installed at the positions indicated by the codifying vector represented in figure 12. The strains to be identified are obtained by developing a virtual test model, subjected to a load condition, represented by a generic combination of parametrized loads. The values of the components in the force vectors are chosen to represent a realistic load condition for the component, which is considered as a segment of a forward spar in a wing in cruise load conditions. The values of internal forces in the wing are used to estimate vertical forces, bending and torsional moments, whereas horizontal loads are separately added. The output of the virtual test model is used to surrogate the vector of the strains acquired by the monitoring system $\{\varepsilon^*\}$, which is introduced in Eq. (5). Once that the number of active sensor is fixed, a Monte-Carlo approach is followed, by randomly varying the codifying vector. For each configuration represented by the codifying vector, the root mean square error (RMSE) and the maximum error (MAXERR) are calculated between the values of the load components identified by the load identification algorithm and the actual values of the load components.

The study is first performed by assuming no discrep-

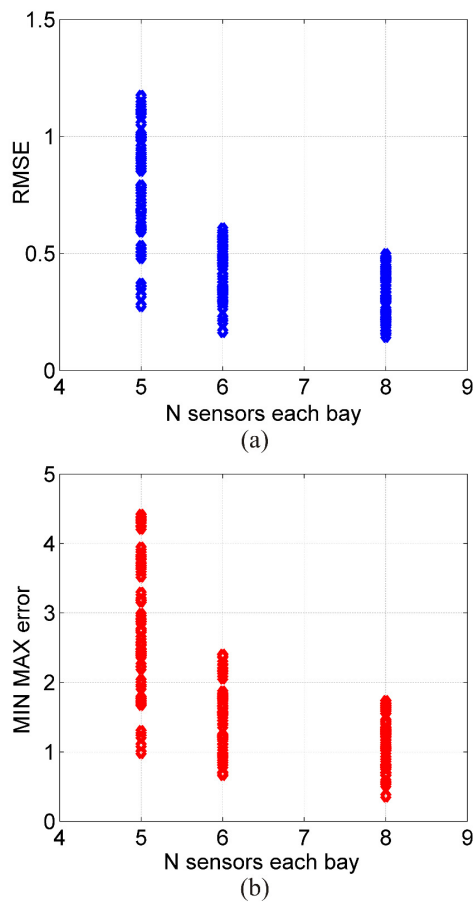


Fig. 14 Load monitoring system performances considering 1000 possible combinations.

anities between the nominal model and the model used for the virtual test. An indication of the system performances is provided in figure 14, where the RMSE and MAXERR indices are given, in percentage, for the best 50 configurations at $n_b = 5, 6, 8$, obtained considering 1000 possible combinations for each n_b value. Load components are identified with a considerable precisions, with RMSE lower than 0.5% and MAXERR lower than 1% for $n_b = 5$. It can be observed that both the indices present minima that progressively decrease as the number of sensor per each bay is reduced. A more realistic situation is considered by introducing differences between the nominal model used to calculate the matrix of influence coefficient and the virtual test model used to surrogate the strains acquired by the sensors. In the virtual test model, the spar segment is divided in 18 sectors, with different lamination sequences obtained by introducing small alteration in the thickness and in the orientation of the plies. Gaussian distributions are considered to attribute the lamination sequence to each sector, with a covariance of 3.6% for the thickness dis-

tribution and of $2deg$ for the distribution of orientation angles with respect to nominal values. The performance of the monitoring system in such conditions is presented in figure 15, where the values of RMSE and MAXERR indices are provided for the best 10 configurations obtained in Monte Carlo approach with 10000 configurations explored for each value of n_b . Although the number of configurations is not adequate to identify optimal performances, results indicate well-defined trends. The number of configurations with acceptable performances is very low with respect to the total number of configurations considered, whereas in the previous case, without discrepancies between nominal and virtual test models, many configurations obtained similar performances. This can be related to the importance of the proper positioning of sensors on the component as well as to a sensitivity to the specific load conditions. The number of sensors has a relevant importance to improve the accuracy of the identified load system. Indeed, Maximum errors are below 27% by using 8 sensors per bay, whereas the RMSE index can be reduced to 11.5% by choosing an adequate sensors configuration. The values of MAXERR are quite high, but it should be noted that such error is typically referred to a force component with a relatively small absolute value, which marginally affects the strain field. In the best configuration found with $n_b = 8$, the MAXERR in the vertical forces, which are the most significant components in the load condition, is of 8.4% and only 4 parameters of the 29 components of the force vector present errors that exceed 18%. Overall, the results of the study presented confirm the possibility to identify with a good detail the complex load conditions in an aeronautical component, provided an adequate number of sensors is used. Hence, the lightness, the reliability and the plainness of installation of the sensor network play a fundamental role to determine the feasibility of such type of monitoring systems. In the presence of uncertainties, the system should be designed considering realistic load conditions and exploring as many configurations as possible to identify the best trade-off between the number of sensor and the robustness of identification.

5 Health monitoring

Modern design philosophies of aircraft structures are nowadays widely adopting damage tolerance fatigue approach, while most up-to-date maintenance procedures are based on predictive concept. Anyhow, if the health condition of the structure (dependent on possible presence of internal damages) is going to be investigated, a large amount of data is needed. As mentioned in the previous section, these data should be acquired in

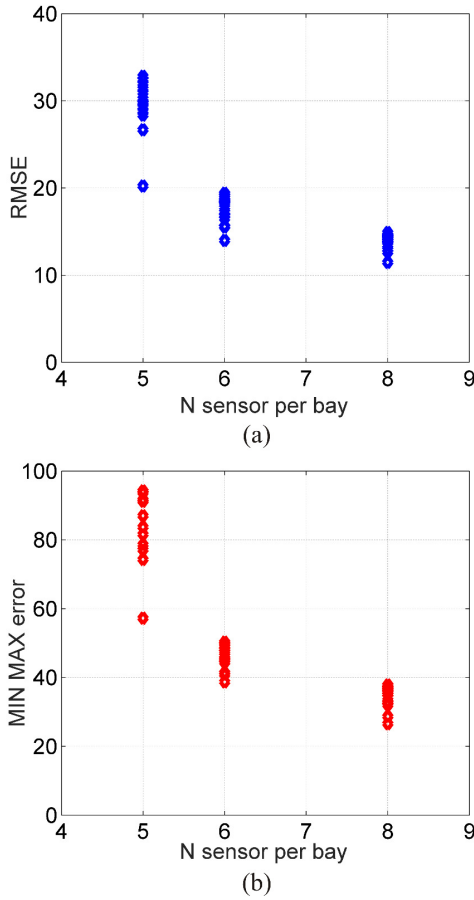


Fig. 15 Load monitoring system performances considering 10000 possible combinations.

real-time, on a continuous time-scale and distributed space-metric. To this purpose, the so called continuous structural health monitoring systems have to be implemented, consisting in a network of sensors able to measure fatigue cracks, corrosion damages, outcomes of low-to-medium energy impacts, technological defects and, in case of composite materials structures, delaminations and honeycomb debondings. The adoption of such structural health monitoring systems allows one to get remarkable savings, in terms of both Direct Operative Costs and, above all, of Direct Maintenance Costs. In modern military aircraft, 44% saving in inspection time is gained thanks to the adoption of these systems in comparison with conventional techniques, as shown in table 1: Among different techniques available for implementing structural health monitoring systems (acoustic-ultrasonic, comparative vacuum monitoring, acoustic emission, sensitive coating, environmental degradation monitoring sensors, microwave sensors, imaging ultrasonic, foil eddy currents), the one based on FO sensors is definitely the more mature and

Table 1 Modern military aircraft: inspection times ([30]).

Type of inspection	Standard duration (% total)	Reduction adopting SHM (% total)	Saved time (% total)
Flight line	16	40	6.4
Scheduled	31	45	14.0
Non scheduled	16	10	1.6
In service	37	60	22.2
Total	100	-	44.0

able to guarantee the best compromise among reliability, sensitivity, low invasivity, quick time-response and acquisition probability [14, 13]. Since the most common damage in composite laminates consists of delaminations, which mainly propagate according to Mode I and Mode II, it appears that, to preliminarily evaluate the efficiency of structural health monitoring systems, double cantilever beam (DCB) and end notched flexure (ENF) fracture mechanics tests should be performed at first [2]. In principle, such an assessment consists in the comparison of FO sensors and electrical strain gauges measurements to FEM analysis results [1]; some typical outcomes of such basic validation tests are reported in figure 16. Load and strain trends, measured as function of crack propagation, allow the investigation of process zone as well the monitoring of strain field evolution. In particular, figure 16b shows that strains, recorded by FBG_{crack} embedded two plies above the pre-cracked central interlaminar layer at 40 mm from the initial crack front, rapidly increase as the crack tip passes below the sensor during DCB tests.

Once demonstrated the capability and reliability of FO sensors to detect strain fields modification due to damage growth in simple standard fracture mechanics coupons, more complex structural components may be considered [3], which are representative of real structural details/subcomponents, like the one reported in figure 17. In this component, the start and evolution of delamination within a T joint has been predicted by numerical simulations and experimentally assessed by embedded FOs. In conclusion, FO sensors-based systems prove to be particularly suited for performing health monitoring of real aircraft structures and able to implement and support damage tolerance fatigue design philosophy and predictive maintenance approach.

6 Process monitoring

Since FO sensors are embedded in composites at lamination stage, they can provide a powerful tool for the monitoring of whole lamination and curing process. In prepreg lamination techniques, (e.g. heated-platen press-

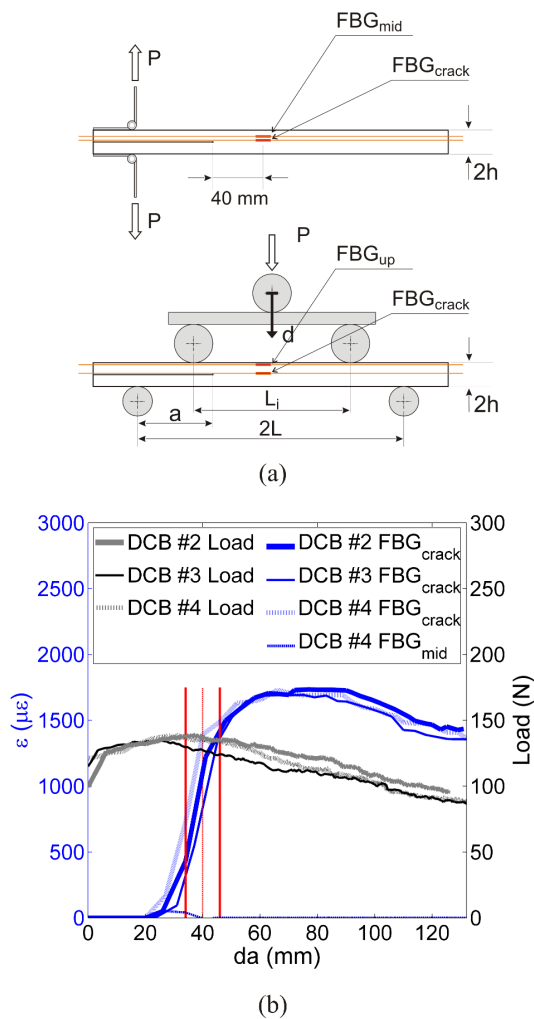


Fig. 16 FO sensors in fracture mechanics tests: (a) test layout and strain sensors location within DCB and ENF specimens; (b) internal strain evolution measured by FBG sensors embedded in DCB specimens. Vertical lines (Fig.16b) identify sensors close to pre-cracked interlaminar layer (FBG_{crack}).

ing and vacuum bag/autoclave), as well as in liquid composite molding, such as RTM, FOs measurements made available since initial stages, allow one to properly choose processing conditions and provide insightful information about manufacturing procedure. Indications about consolidation, resin curing progression, composite temperature evolution, final residual strains can be gathered from the output signal of embedded FBGs [25]. Moreover, in case of liquid resin processes (RTM, resin infusion, etc.) additional information can be obtained about resin flow rate, preferential paths, incomplete mould filling, presence of dry spots. For these last purposes, standard FOs (with no FBGs) may be employed, which are considerably cheaper and can be easily embedded [16, 18]. A further interesting use of FBG sensors becomes apparent in case of adhesive joining,

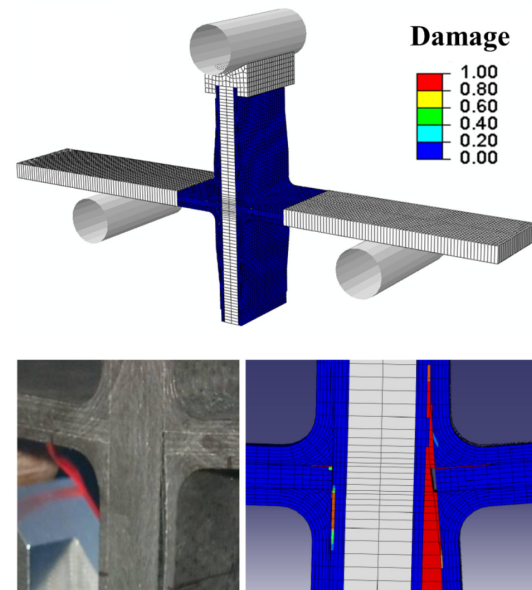


Fig. 17 Complex structural composite component for FO health monitoring applications.

where local temperature/strain evolution during adhesive cure can be monitored. It should be noted that all such data are obtained in real-time and give a direct indication of what is occurring within the laminate or the adhesive layer. To acquire FOs signals since the beginning of technological process, adaptation of moulds and manufacturing equipment may be required. In case of vacuum bag/autoclave processes, long portions of fibers protruding from the laminate must be left, to allow an easy connection to opto-electronics. Once sensing fibres are embedded into laminate, proper passages through vacuum bag sealing and special by-passes should be employed to drive FOs signal out of autoclave. Moreover, in case of heated platen pressing, suitable adaptation of mould edges may be required, not to damage FOs protruding from laminate during part de-moulding. Special care must be taken in RTM process as well, mainly in case of vacuum-assisted resin injection technology. As a matter of fact, mould vacuum tightness is crucial to guarantee the final quality of moulded components. Even slight vacuum losses lead to air leakage in the mould and consequent incomplete reinforcement wetting; so protruding fibers should be placed within soft seals granting air and pressure tightness during the whole mould filling stage (Fig.18). These drawbacks often represent the limiting issues for a wider adoption of FO sensors in process monitoring. Figure 18 reports the information supplied by three plain optical fibres placed at different distance from the inlet of a RTM mould during resin injection in a preform. Signal drop, due to abrupt refractive index variation, occurs when resin

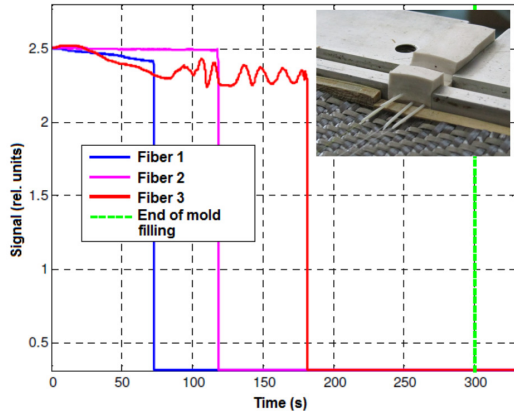


Fig. 18 Signals from three optical fibres in a RTM preform during resin injection.

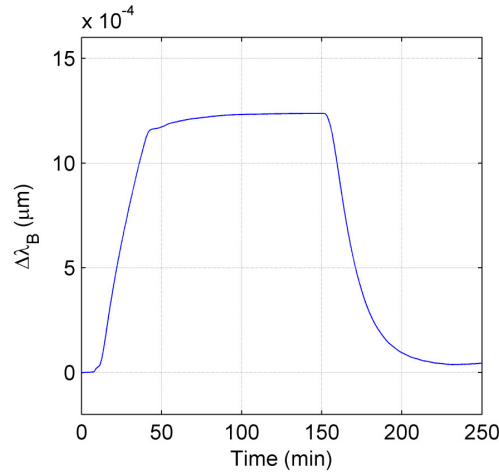


Fig. 19 Signal from a FBG embedded in the adhesive layer of an hybrid joint.

reaches optical fibres tip. Actual resin flow rate can easily be calculated. As it will be shown in section 7, FBGs signal wavelength is related to material strain and temperature. Figure 19 shows such wavelength variation occurring when a FBG sensor is embedded into the adhesive layer during the hot curing stage of an hybrid joint. Further information about adhesive temperature time-history and final residual strains can be gathered as well.

7 Decoupling techniques of thermal and mechanical effects

In the previous sections, it has been shown that, once solved technological concerns relevant to embedment, invasivity and stress-transfer capability, FO sensors are particularly suited to load, health and process moni-

toring of composite structures, provided efficient techniques are adopted for decoupling thermal and mechanical effects. As a matter fact, FBG sensors based on uniform Bragg gratings, allow the measurement of deformations and temperature through the variation of reflected wavelength. According to the well-known Bragg's relationship (6) among wavelength (λ_B), effective refractive index (n_{eff}) and grating period (Λ), signal variation $\Delta\lambda_B$ depends on both thermal and mechanical effects according to Eq. (7) [33]:

$$\lambda_B = 2n_{eff}\Lambda \quad (6)$$

$$\Delta\lambda_B = \lambda_B(1 - p_e)\varepsilon_1 + \lambda_B(\alpha_{CTE} + \zeta)\Delta T \quad (7)$$

where photo-elastic p_e and thermo-optic coefficients ζ represent respectively strain and temperature dependence on refractive index, α_{CTE} is FOs thermal expansion coefficient, ε_1 and ΔT refer to strain and temperature variations. Finally, introducing the coefficients of proportionality K_ε and K_T , Eq. (7) can be expressed as:

$$\Delta\lambda_B = K_\varepsilon\varepsilon + K_T\Delta T \quad (8)$$

Referring to Eq. (8), a few techniques based on the following Eqs. (9) have been proposed.

$$\begin{Bmatrix} \Delta\lambda^1 \\ \Delta\lambda^2 \end{Bmatrix} = \begin{bmatrix} K_\varepsilon^1 & K_T^1 \\ K_\varepsilon^2 & K_T^2 \end{bmatrix} \begin{Bmatrix} \varepsilon \\ \Delta T \end{Bmatrix} \quad (9)$$

By means of two distinct FBG sensors inscribed on FOs having different cross section, James S.W. et al. [23] and Frazo O. et al. [28, 15], developed a system relying on the different response provided by different sensors when the same stress is applied. Such a technique is presented by Jin L. et al. [24]. As an alternative, the convenience to embed a portion of the sensor into different materials is proposed by Guan B. O et al. [20]. Few techniques are particularly suitable when FO sensors embedded into composite laminates. Udd E. et al. [32] adopted a couple of FBGs having different Bragg's wavelengths inscribed on the same stretch of fibre. Yam P. et al. [34] proposed to decouple the signal by means of sensors characterized by a phase-shifted response (π -shifted). An alternative measurement system, adopting sensors generated by particular phase masks, is proposed by Caucheteur C. et al. [11], which uses tilted sensors. Being not perpendicular to FO axis, part of the signal is transmitted to FO cladding, thus obtaining a wavelength whose value depends on the characteristics of both core and cladding. Based on the use of capillary tubes, two simple decoupling techniques are proposed and tested [9]. The first one (*Extremity Capillary Tube - ECT technique*), complies to what proposed by Montanini and D'Acquisto

[27]. It accomplish signal decoupling by directly embedding a uniform Bragg grating (FBG1) into composite structure, while a second standard sensor (FBG2), inscribed at the extremity of a FO, is loosely inserted in a capillary tube, also embedded in the laminate. These sensors react differently to thermal and mechanical stimuli, since FBG1 response is influenced by temperature and host material deformation (due to both mechanical and thermal effects), while FBG2, which is loose inside capillary, feels only thermal effects. The proportionality coefficients K_ε in Eq. (9) can be written as:

$$\begin{aligned} K_\varepsilon^1 &= \lambda_B^1 (1 - p_e) \\ K_\varepsilon^2 &= 0 \end{aligned} \quad (10)$$

The gratings response to temperature variations is different as well, since the change of wavelength of the sensor directly embedded is affected by the thermal deformation of the whole structure, not only by that of optical fibre. The two proportionality coefficients K_T can be written as:

$$\begin{aligned} K_T^1 &= \lambda_B^1 (\zeta + \alpha_{ris}) \\ K_T^2 &= \lambda_B^2 (\zeta + \alpha_{FO}) \end{aligned} \quad (11)$$

where α_{ris} represents thermal expansion of the composite/embedded fibres system, which can be obtained by a micro-mechanical analysis. The alternative technique (*Across Capillary Tube - ACT*) overcomes the problem of multiplexing downstream capillary, since the fibre is not interrupted. ACT relies on a first sensor (FBG1) directly embedded into composite, while the second sensor (FBG2) is inscribed on a continuous optical fibre, loosely constrained inside a capillary. As a consequence, the optical fibre assumes a curvy shape inside the capillary, whose elongation does not implies a corresponding deformation of FBG2. The re-sponse of FBG2 to applied external strains is not null, but sensibly differs from that of FBG1. However, the response of FBG2 ($K^2 \neq 0$) varies according to the

applied deformation. For small strains, the strain coefficient is assumed to be constant and the equation (9) allows a correct estimation of thermal/mechanical effects [9]. Fig.20 reports the calibration curves relevant to *ECT technique* obtained by separately imposing strain or temperature variations. They show different responses of FBG sensors to thermal and mechanical stimuli. The linearity of such responses allows one to determine all matrix components in Eqs. 9, as well as to solve the system. Figure 21 reports the results of validation tests, consisting in simultaneous temperature and strain variations applied to a composite coupon. The comparison of FBGs, electrical strain gages and thermocouples outcomes assesses the reliability of **ECT decoupling technique**.

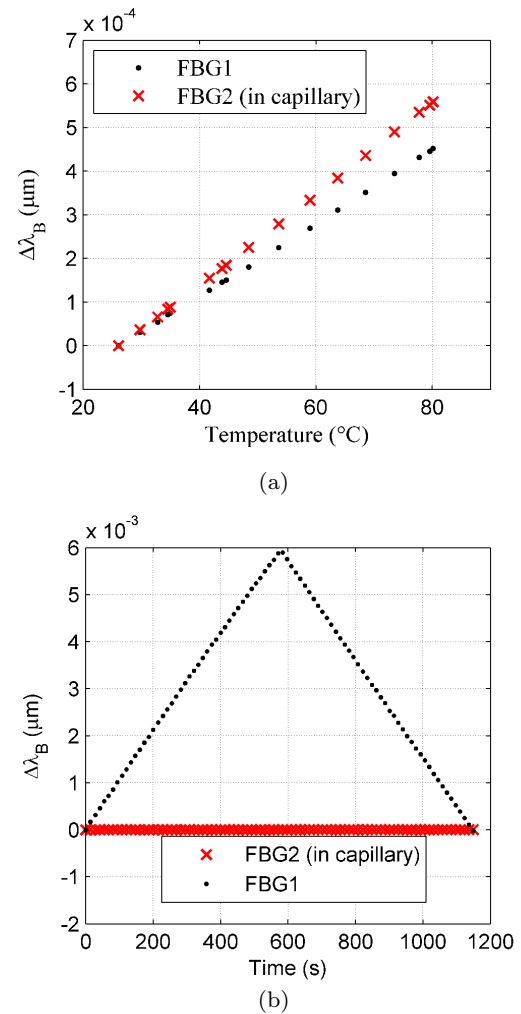


Fig. 20 Application of *ECT technique* to thermo-mechanical decoupling of FBG signal: (a) Temperature; (b) deformation response of sensors during calibration tests.

8 Strain field reconstruction from FO sensors spectra

In section 4 an inverse problem is dealt with, devoted to the reconstruction of the whole strain field in a structural element on the basis of local strain measured by standard FBG sensors. In the following, another kind of inverse problem, typical of FO monitoring system, is solved, which allows one to obtain the global strain field starting from optical spectra got by special FO sensors. As a matter of fact, the wavelength of the reflection spectrum for a chirped FBG has a one-to-one correspondence to the position along the gauge section, thus allowing strain reconstruction over the entire sensor length. In particular, *Draw Tower Grating* sensors are particularly appealing since they can provide a strain field over an extended spatial region. The first step to develop a strain reconstruction tool consists in the im-

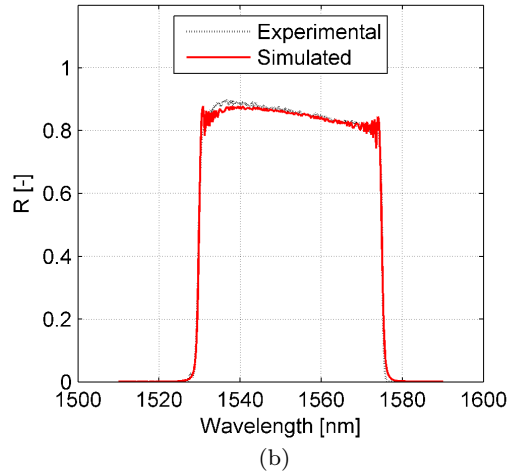
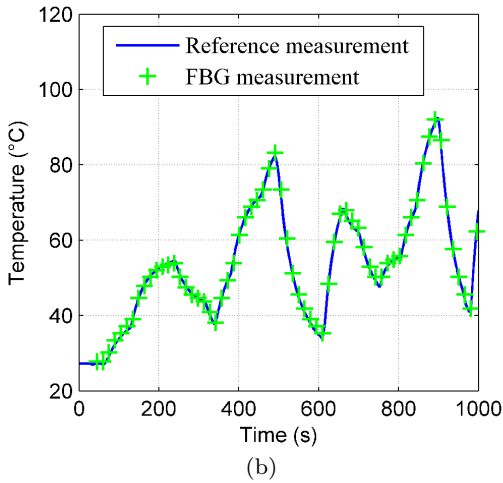
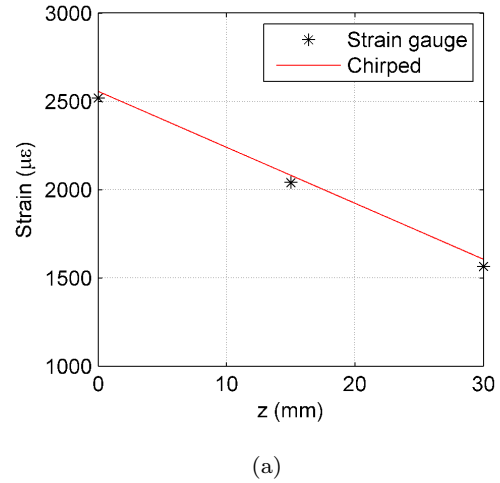
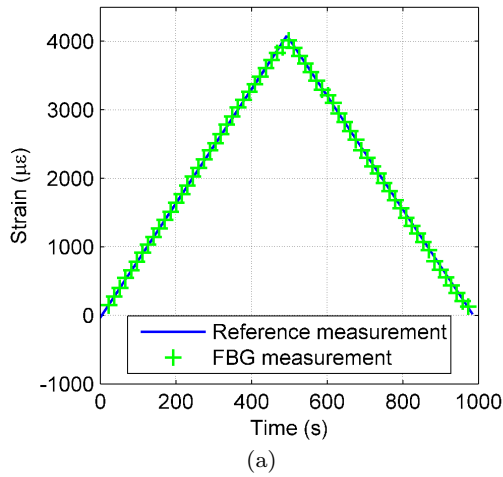


Fig. 21 Application of *ECT technique* to thermo-mechanical decoupling of FBG signal: validation tests.

Fig. 22 Chirped sensor: (a) numerically-reconstructed strain profile compared to experimental one; (b) corresponding spectra; linear strain test case; maximum strain level 2500 μm .

plementation of an algorithm simulating the reflected spectrum of a sensor subject to an arbitrary deformation profile. Then, such algorithm has to be coupled to an optimization procedure which finds the strain profile minimizing the difference between simulated and experimental spectra [29, 37]. A grating simulation approach relying on the Coupled Mode Theory (simplified theory derived from Maxwell's equations [26]) is reported in detail in [10], where TMM (Transfer Matrix Method) is exploited as well, together with an optimization technique based on a hybrid genetic algorithm. To validate such a strain reconstruction tool, tests are performed on chirped grating sensors. To check repeatability and robustness, several cases are investigated for each shape of strain profile, with increasing deformation magnitude. Strain gauges are located close to sensors edges in order to monitor the actual strain distribution. Once completed the apodization process (applied

to reflected spectrum of unloaded sensor) to identify the apodization profile, such apodized profile can be used for simulating the reflected spectrum of loaded sensor (Fig.22a) and for reconstructing the strain field, as reported in figure 22b. As an alternative, *Draw Tower Grating* arrays can be considered. They present several advantages over traditional arrays, e.g. allowing several different combination of spectral and spatial characteristics. To identify the best combination for strain reconstruction applications, three of them are considered, every array being composed of 10 individual FBG sensors[10]:

- Spatial continuity and spectral discontinuity (*SpaC/SpED*):
Each sensor is 10 mm long; no spatial separation exists between two adjacent gratings. Sensors wavelength are separated by 1 nm;

- Spatial continuity and spectral continuity (*SpaC/SpC*): Spatial configuration as *SpaC/SpD*. Individual sensors wavelength separation is 0.1 nm, that is the Full Width Half Maximum of a single peak. Resulting spectrum is continuous, with local maxima corresponding to each FBG Bragg's wavelength;
- Spatial discontinuity and spectral continuity (*SpaD/SpC*): 3 mm long sensors, 7 mm spatial separation between two adjacent gratings. Wavelength separation is $\leq FWHM$ originating a continuous reflection spectrum. No local maxima are present, given the greatest width of the individual peaks.

Spectral discontinuity allows individual peak tracking and consequently real-time monitoring. However, to allow wavelength division multiplexing, the number of single FBG which can be inscribed on the FO should be limited; moreover, peak tracking gives no information about strain gradients. Spectral continuity generates narrower spectra, but requires spectral analysis and makes it impossible to perform real-time monitoring. Likewise chirped grating case, several tests should be performed for obtaining different strain profiles. However, being *Draw Tower Grating* arrays longer than chirped ones, more complex strain profiles can be applied: uniform, linear, triangular and quasi-quadratic distribution. In the following, some typical results (reconstructed spectra and strain profiles) are reported, respectively relevant to *SpaC/SpD* and *SpaD/SpC* cases (Fig.23 and Fig.24). Sensors are bonded to aluminum coupons, together with reference strain gauges positioned in correspondence of each individual grating.

9 Conclusion

This paper faces a particular aspects of one crucial issues of continuous mechanics, that is the experimental investigation of stress- and strain field inside materials and structures. Specifically, an overview is presented, dealing with FOs monitoring systems applied to aeronautical structures design, production and management. Main features and drawbacks are considered as far as integration and networking issues are concerned. FO sensors networks allow one to perform distributed or point-to-point acquisition, exploiting multiplexing techniques based on Wavelength or Time Division Multiplexing approaches, depending on structure dimensions and type of analysis (static or dynamic). Other aspects of paramount importance are represented by attenuation, thermal-mechanical coupling, degree of network fractioning and consequent reliability, main-

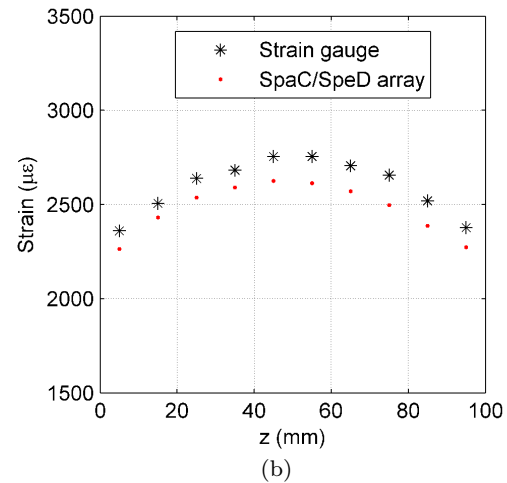
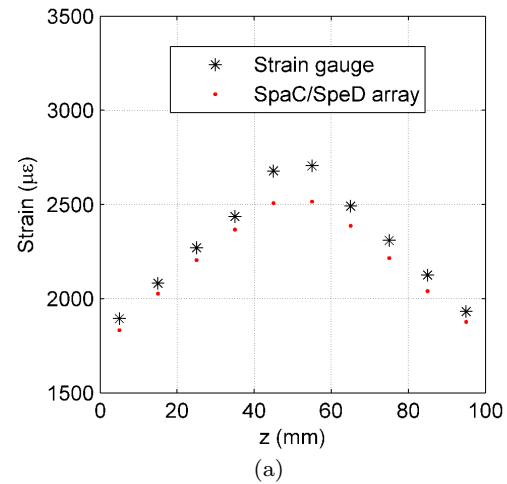


Fig. 23 *Draw Tower Grating* array in SPATial Continuity and SPEctral Discontinuity (*SpaC/SpD*) configuration: strain reconstruction via individual peak tracking. (a) Lin-ear strain with gradient change test case; (b) quasi-quadratic strain test case.

tainability, reparability, complexity, weight and cost. More specifically, fibres integration into a host material can be performed through bonding or embedding, both choices implying advantages and drawbacks. The interface between fibre and host material deserves special attention, as well as the role played by connectors and, in general, possible effects due to invasivity. However, FO sensors-based systems prove to be particularly efficient in load, health and process monitoring. In particular, a detailed knowledge of load conditions acting in an aircraft main structural component can provide crucial data to set-up maintenance operations. Besides, the continuous monitoring of structural response can allow the detection of load paths modification, due to structural ageing or damage onset. In addition, since modern fatigue design techniques are

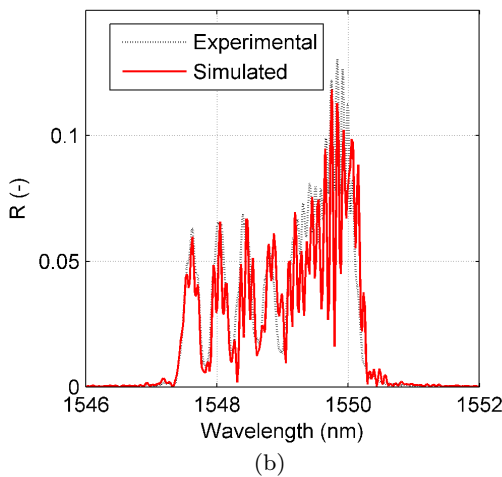
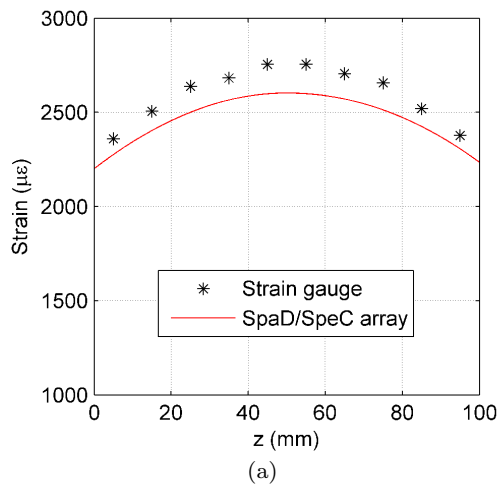


Fig. 24 Draw Tower Grating array in SPAtial Discontinuity and SPEctral Continuity (*SpaD/SpaC*) configuration: (a) numerically reconstructed strain profile compared with the experimentally applied one; (b) corresponding spectra. Quasi-quadratic distribution strain profile test case.

widely adopting the damage tolerance approach, while the most up-dated maintenance philosophies are based on the predictive concept, a huge amount of data relevant to structural health is required. Such real-time information should be made available in a continuous and distributed way: FO networks represent the best compromise among sensitivity, promptness, low invasivity and reliability. Finally, in case of structures made of composite materials, FO sensors can represent a powerful tool for the monitoring of the whole lamination and curing process. In case of vacuum bagging, resin transfer moulding and bonding techniques, indications about consolidation, resin curing progression, temperature evolution and final residual stresses can be gathered from FO sensors. Since these sensors are then left inside the composite structural element for in-service

load and health monitoring, a real from-the-cradle-to-the-grave strategy can be put in place. The paper also shows that the use of FBG sensors, together with proper strain reconstruction codes, can represent a significant step forward in developing complete SHM systems. In particular, chirped gratings provide excellent results for simple strain profiles, but, being post-processing extremely time consuming, this approach is may be not adequate for real-time monitoring. Three configurations of DTG arrays are tested as well [10]. *SpaC/SpaD* configuration can identify strains via direct peak tracking, but numerical reconstruction proved to be unsuccessful. Similar problems arose for *SpaC/SpaC* configuration; in addition, direct peak tracking is impossible. On the contrary, through *SpaD/SpaC* configuration, numerical reconstruction procedure is successfully performed in every load case. In conclusion, numerical strain reconstruction tools can be profitably applied to FBGs arrays having suitable spectral characteristics. A further issue faced by the paper refers to experimental techniques for decoupling thermal and mechanical effects affecting embedded FBG sensors. Decoupling techniques provide reliable correspondence between measured strains/temperatures, requiring only small capillaries and so limiting expected invasivity. In general invasivity of both techniques can be reduced adopting short FBGs (e.g. 1mm) smaller FOs (e.g. 50µm diameter).

Acknowledgements The sponsorship of MIUR and Regione Lombardia within the frame of STIMA, SMAT and MACH projects are gratefully acknowledged. The experimental activities described in this paper have been performed at Advanced Materials Laboratory (AMALA) of Politecnico di Milano.

References

1. Airoldi A, Sala G, Bettini P, Baldi A (2013) An efficient approach for modeling interlaminar damage in composite laminates with explicit finite element codes. *Journal of Reinforced Plastics and Composites* 32(15):1075–1091
2. Airoldi A, Baldi A, Bettini P, Sala G (2014) Efficient modelling of forces and local strain evolution during delamination of composite laminates. *Composites Part B: Engineering*
3. Baldi A, Airoldi A, Crespi M, Iavarone P, Bettini P (2011) Modelling competitive delamination and debonding phenomena in composite t-joints. *Procedia Engineering* 10:3483–3489
4. Barbarino S, Bilgen O, Ajaj RM, Friswell MI, Inman DJ (2011) A review of morphing aircraft. *Jour-*

- nal of Intelligent Material Systems and Structures 22(9):823–877
5. Bettini P, Sala G (2008) Preliminary assessment of helicopter rotor blades fatigue endurance through embedded fo sensors. In: Proceeding of the 24th ICAF Symposium, pp 16–18
 6. Bettini P, Riva M, Sala G, Di Landro L, Airoidi A, Cucco J (2009) Carbon fiber reinforced smart laminates with embedded sma actuators part i: Embedding techniques and interface analysis. *Journal of materials engineering and performance* 18(5-6):664–671
 7. Bettini P, Di Landro L, Airoidi A, Baldi A, Sala G (2011) Characterization of the interface between composites and embedded fiber optic sensors or nitinol wires. *Procedia Engineering* 10:3490–3496
 8. Bettini P, Bertoli S, Sala G, Gaspari R, Pozzati G (2012) Development of state-of-the-art optical sensors for the monitoring of deep sea umbilicals and flexible pipelines. In: *SPIE Smart Structures and Materials + Nondestructive Evaluation and Health Monitoring*, International Society for Optics and Photonics, pp 83,430E–83,430E
 9. Bettini P, Sala G, Di Landro L, Tessadori E (2012) Embedded fibre optic techniques for primary structural components: Strain and temperature monitoring. In: *Proceedings of the 15th European Conference on Composite Materials, ECCM, Padova (It), ICCM*
 10. Bettini P, Guerreschi E, Sala G (2015) Development and experimental validation of a numerical tool for structural health and usage monitoring systems based on chirped grating sensors. *Sensors* 15(1):1321–1341
 11. Caucheteur C, Chen C, Albert J, Mégret P (2006) Use of weakly titled fiber bragg gratings for strain sensing purposes. In: *Proceedings Symposium 2006, Eindhoven, The Netherlands*
 12. Chojetzki C, Rothhardt M, Ommer J, Unger S, Schuster K, Mueller HR (2005) High-reflectivity draw-tower fiber bragg gratings arrays and single gratings of type ii. *Optical Engineering* 44(6):060,503–060,503
 13. Ciminello M, Bettini P, Ameduri S, Guerreschi E, Cuneo G (2014) Experimental validation of a sensorized ring based on optical fiber for strain monitoring of morphing structure. In: *29th International Council of the Aeronautical Sciences (ICAS 2014)*, International Council of the Aeronautical Sciences, DEU, pp 1–10
 14. Ciminello M, Bettini P, Ameduri S, Guerreschi E, Concilio A, Sala G (in press) Monito-ring: an original fo system for morphing application. *Journal of Intelligent Material Systems and Structures*
 15. Frazão O, Marques L, Marques J, Baptista J, Santos J (2007) Simple sensing head geometry using fibre bragg gratings for strain–temperature discrimination. *Optics Communications* 279(1):68–71
 16. Gerosa R, Stefania G, Tagliabue P, Bettini P, Di Landro L (2009) Monitoring of vartm process by embedded fiber optics. In: *Atti del XX Congresso Nazionale AIDAA, Milano (It), AIDAA*, pp 1–9
 17. GMBH FT (2015) FBGS Draw Tower Gratings. <http://www.fbgs.com/>, [Online; accessed 05-March-2013]
 18. Grande AM, Di Landro L, Bettini P, Baldi A, Sala G (2011) Rtm process monitoring and strain acquisition by fibre optics. *Procedia Engineering* 10:3497–3502
 19. Grattan K, Sun T (2000) Fiber optic sensor technology: an overview. *Sensors and Actuators A: Physical* 82(1):40–61
 20. Guan BO, Tam HY, Chan HL, Choy CL, Demokan MS (2002) Discrimination between strain and temperature with a single fiber bragg grating. *Microwave and optical technology letters* 33(3):200–202
 21. Hagemann V, Trutzel M, Staudigel L, Rothhardt M, Müller HR, Krumpholz O (1998) Mechanical resistance of draw-tower-bragg-grating sensors. *Electronics Letters* 34(2):211–212
 22. Jackson S (2002) Systems engineering for commercial aircraft. Aldershot
 23. James S, Dockney M, Tatam R (1996) Simultaneous independent temperature and strain measurement using in-fibre bragg grating sensors. *Electronics Letters* 32(12):1133–1134
 24. Jin L, Zhang W, Zhang H, Liu B, Zhao J, Tu Q, Kai G, Dong X (2006) An embedded fbg sensor for simultaneous measurement of stress and temperature. *Photonics Technology Letters, IEEE* 18(1):154–156
 25. Kang HK, Kang DH, Bang HJ, Hong CS, Kim CG (2002) Cure monitoring of composite laminates using fiber optic sensors. *Smart Materials and Structures* 11(2):279
 26. Kashyap R (1999) *Fiber bragg gratings*. Academic press
 27. Montanini R, dAcquisto L (2007) Simultaneous measurement of temperature and strain in glass fiber/epoxy composites by embedded fiber optic sensors: I. cure monitoring. *Smart Materials and Structures* 16(5):1718
 28. Romero R, Frazão O, Pereira D, Salgado H, Araújo F, Ferreira L (2005) Intensity-referenced and temperature-independent curvature-sensing con-

- cept based on chirped fiber bragg gratings. *Applied optics* 44(18):3821–3826
29. Rostami A, Yazdanpanah-Goharriz A (2007) A new method for classification and identification of complex fiber bragg grating using the genetic algorithm. *Progress In Electromagnetics Research* 75:329–356
30. Staszewski W, Boller C, Tomlinson GR (2004) *Health monitoring of aerospace structures: smart sensor technologies and signal processing*. John Wiley & Sons
31. Tessler A, Spangler JL (2005) A least-squares variational method for full-field reconstruction of elastic deformations in shear-deformable plates and shells. *Computer methods in applied mechanics and engineering* 194(2):327–339
32. Udd E, Kreger S, Calvert S, Kunzler M, Davol K (2003) Usage of multi-axis fiber grating strain sensors to support nondestructive evaluation of composite parts and adhesive bond lines. Tech. rep., DTIC Document
33. Wang Y, Han B, Kim D, Bar-Cohen A, Joseph P (2008) Integrated measurement technique for curing process-dependent mechanical properties of polymeric materials using fiber bragg grating. *Experimental Mechanics* 48(1):107–117
34. Yam SP, Baxter GW, Wade SA, Collins SF (2010) Modelling of an alternative pi-phase-shifted fibre bragg grating operating at twice the bragg wavelength. In: 35th Australian conference on optical fibre technology, Australian Institute of Physics
35. Yashiro S, Takeda N, Okabe T, Sekine H (2005) A new approach to predicting multiple damage states in composite laminates with embedded fbg sensors. *Composites Science and Technology* 65(3):659–667
36. Zhandarov SF, Pisanova EV (1997) The local bond strength and its determination by fragmentation and pull-out tests. *Composites Science and Technology* 57(8):957–964
37. Zhang R, Zheng S, Xia Y (2008) Strain profile reconstruction of fiber bragg grating with gradient using chaos genetic algorithm and modified transfer matrix formulation. *Optics Communications* 281(13):3476–3485